Tampereen yliopisto

Ella Lampela

ENGINEERED SKELETAL MUSCLE BUNDLES – OPTIMIZATION OF 3D IMAGING PROTOCOLS

Faculty of Medicine and Health Technology (MET)
Bachelor's thesis
April 2021

TIIVISTELMÄ

Ella Lampela: “Kudosteknologiset luurankolihassolukimput – 3D-kuvantamisprotokollien optimointi”
Kandidaatin tutkielma
Tampereen yliopisto
Bioteknologian ja biolääketieteen tekniikan tutkinto-ohjelma
Huhtikuu 2021

Luurankolihas on ihmiselimistön uusiutumiskykyisin ja runsain kudos. Se on heterogeeninen, toistensa kanssa linjassa olevien ja monitumaisten lihassolujen, eli lihassyiden (engl. *myotube*), muodostama rakenne. Luurankolihas on kudosteknologian saralla kasvavan kiinnostuksen kohteena. Toinen ajankohtainen aihe kudosteknologiassa on kantasolujen käyttö kudosteknologisten menetelmillä toteutetuissa tukirakenteissa.

Mesenkymaalisilla kantasoluilla (MSC) viitataan olevan muuntautumiskykyä monilinjaiseen erilaistumiseen, samoin kuin kyky muodostaa monitumaisia lihassyitä sulautumalla yhteen myogeenisten solujen kanssa. Näitä kutsutaan hybridilihassyiksi. Tutkimukset esittävät, että viljeleminen yhdessä myogeenisten solujen kanssa edistää mesenkymaalisten kantasolujen erilaistumista kohti myogeenista linjaa ja yhteensulautumista lihassyiksi. Rasvasta eristettyjen mesenkymaalisten kantasolujen on esitetty olevan kyvykkäitä erilaistumaan myogeenisen linjan mukaan.

Luurankolihaksen kudosteknologinen toteuttaminen kolmiulotteisena hyödyntää erikoisvalmisteista muottia, joka luo rakenteeseen mekaanisen vetojänniteen. Tämä jännite järjestää solut suuntautumaan voiman suuntaisesti, luoden järjestelmällisen morfologian, joka voidaan havaita tämän tutkimuksen tuloksissa esitetyistä kuvista. Kolmiulotteisten koeasetelmien ja -näytteiden tulosten esittäminen asettaa vaatimuksen kolmiulotteisesta kuvarekonstruktiosta. Siksi värjäysprotokollien, kuvantamisen ja esitysmuodon optimointi korkealaatuisen kolmiulotteisen rekonstruktion tuottamiseksi on tarpeellista.

Tämän tutkimuksen tavoitteena on parantaa ihmisen rasvakudosperäisten kantasolujen tumien luotettavaa paikantamista lihassyiden sisällä viljeltäessä yhdessä C2C12-solujen kanssa. Tumien luotettava lokalisointi lihassolurakenteiden sisällä nostaa yhteensulautumissuhteen (engl. *fusion ratio*) määrittämistä.

Kolmiulotteisten kuvien laatua kohennettiin värjäyksen toistokertojen ja digitaalisen parantamisen kautta tasolle, jossa kolmiulotteisen datan kvantitatiivinen analyysi voi alkaa, ja näköön perustuva fuusion arvioiminen ja tumien lokalisointi lihassyiden sisälle oli mahdollista.

Avainsanat: rasvakudoksesta peräisin olevat kantasolut, mesenkymaaliset kantasolut, kudosteknologinen luurankolihas, lihassyy, hybridilihassyy, luurankolihassolu, konfokaalikuvantaminen, immunovärjäys, vasta-ainevärjäys, immunohistokemia, immunosytokemia, ihmisen tumien värjääminen, biolääketieteen teknologia, kantasolujen biologia, kudosteknologia

Tämän julkaisun alkuperäisyys on tarkastettu Turnitin OriginalityCheck –ohjelmalla.

ABSTRACT

Ella Lampela: ”Engineered Skeletal Muscle Bundles – Optimization of 3D Imaging Protocols”
Bachelor’s thesis
Tampere University
Degree Programme in Biotechnology
April 2021

Skeletal muscle is the most regenerative and abundant tissue of the human body, a heterogenous structure formed by aligned and multinucleated myotubes. It is a growing target of interest in the field of tissue engineering. Another topical interest in the field is using stem cells in engineered scaffold structures.

Mesenchymal stem cells (MSCs) are indicated to have multilineage differentiation potential, as well as the ability to fuse with myogenic cells to create multinucleated myotubes (called hybrid myotubes). Studies suggest that coculturing MSCs with myogenic cells promotes the differentiation of MSCs towards myogenic lineage and their fusion into myotubes. Adipose-derived mesenchymal stem cells are indicated to potentially differentiate along the myogenic lineage.

Engineering three-dimensional (3D) skeletal muscle structures utilizes a specially engineered mold, which creates a traction force lining the cells along the mechanical strain creating an oriented morphology which can be observed from the figures presented in the results of this study. When displaying results of three-dimensional experiment setups and samples, 3D image reconstruction and quantitative analysis of all three dimensions is necessary. Therefore, optimizing the staining protocol, imaging and presentation format for high-quality 3D reconstructed images is needed.

The aim of this study is to improve the reliable detection of human adipose-derived stem cell (ASC) nuclei inside the myotubes when cocultured with mouse C2C12 cells. The reliable localization of nuclei inside the myotubes improves the reliability of fusion ratio determination.

The 3D image resolution was enhanced through staining iterations and digital enhancing to a level, where quantitative 3D data analysis can begin, and the visual localization of nuclei inside the myotubes was possible.

Keywords: adipose-derived stem cell, mesenchymal stem cell, engineered skeletal muscle, myotube, hybrid myotube, confocal imaging, immunostaining, immunohistochemistry, immunocytochemistry, human nuclei staining, biomedical engineering, stem cell biology, tissue engineering

The originality of this thesis has been checked using the Turnitin OriginalityCheck –program.

ACKNOWLEDGEMENTS

This Bachelor's thesis study has been conducted in the Susanna Miettinen's Adult Stem Cell group in Tampere University.

I thank Sari Kalliokoski, Maija Kauppila and Laura Honkamäki for valuable tips and help with sample preparation protocols. Lassi Sukki and Kaisa Tornberg from Pasi Kallio's research group provided us with the custom molds for this study. I thank Sanna Korpela for introducing me to confocal imaging and Sari Toivola for the introduction to immunohistochemistry. I am increasingly grateful for Toni Montonen for vital advice and help with the imaging units and deconvolution software.

I would like to thank Susanna Miettinen for giving me this opportunity in the research group. I express my gratitude to my supervisor Miina Björninen, who introduced me to the fascinating topic of skeletal muscle engineering with mesenchymal stem cells, and who has tirelessly guided this study and directed me in my writing process.

Lastly, warm gratitude needs to be expressed to my loved ones, who keep my feet on the ground.

Tampere, 27.4.2021

Ella Lampela

CONTENTS

1. INTRODUCTION

Tissue engineering continues its search towards meeting the growing need for vital replacement tissues and organs. One of the typical approaches in tissue engineering is the usage of stem cells cultured in an engineered scaffold structure (Stock, Vacanti, 2001).

Skeletal muscle is the most regenerative and abundant tissue in the human body (Tedesco et al., 2010, Rao et al., 2018). It is formed by multinucleated myotubes which in turn is formed by cells elongating, aligning, and fusing together (Kocaefe et al., 2010). In their review article, Schiaffino and Reggiani highlight the muscle fiber heterogeneity as the foundation of its ability to perform low-intensity activity, repeated submaximal contractions as well as maximal contractions (Schiaffino, Reggiani, 2011).

Using stem cells of human origin in both skeletal muscle clinical and research applications is desirable for various reasons. Autologous transplants (in which both the graft donor and host are the same individual) replacing degenerated tissues or organs minimizes the unwanted response from adaptive immune system (Burdzińska et al. 2008). Current methods for human skeletal muscle disease modeling resort to two-dimensional (2D) (Beier et al., 2011, Di Rocco et al., 2006, Huang et al., 2005) and animal models. A reliable manifestation of function and responsiveness in human skeletal muscle requires improvement from the current approach. An ideal tissue engineered product would include a sustainable stem cell source that can be expanded into large amounts *in vitro,* as well as organize into a three-dimensional (3D) structure. This would require a viable resource of myogenic progenitor cells and 3D culturing conditions facilitating the stimulation of contractile functions. Taking these measures would ideally result in functional, 3D force-generating muscle constructs (Rao et al., 2018). Though primary skeletal muscle cells can be obtained through biopsies, yielding stem cells would enable a larger donor population, thanks to the stem cells' ability to renew themselves without differentiation (Truskey, 2018, Burdzińska et al., 2008, Alberts et al., 2015). Functional engineered skeletal muscle tissues have been reported in the recent years (Rao et al., 2018).

Many studies revolving around engineered skeletal muscle concentrate on induced pluripotent stem cells (iPSCs) (Truskey, 2018, Rao et al., 2018), while similar studies utilizing mesenchymal stem cells (MSCs) are fewer in number (Torres-Torrillas et al., 2019, Gang et al., 2004, Wakitani et al.,1995). MSCs have been indicated to show differentiation potential along multiple lineages, such as those of adipocytes, chondrocytes, myocytes, osteocytes and neurocytes (Zuk et al., 2001, Battula et al., 2007, Beier et al., 2011). MSCs obtained from adult donors surpass many of the obstacles considering availability and ethics (Gimble, Guilak, 2003), as described in the following chapter.

MSCs are most abundant in the adipose tissue and are therefore relatively simple and affordable to acquire with relatively non-invasive methods. Some studies report that adipose-derived mesenchymal stem cells, briefly adipose stem cells (ASCs), have shown differentiation potential towards myogenic (Di Rocco et al., 2006) and neuronal (Safford et al., 2002) lineages. Therefore, they are a potential source for skeletal muscle tissue engineering. *Figure 1.* displays the differentiation of myotubes from satellite cells, which are resident stem cells positioned between the basal lamina and sarcolemma of a myofiber (Pasut, Jones & Rudnicki, 2013, Zouraq et al., 2013). Some of the essential myogenic differentiation markers expressed in each phase are presented. In addition to their capacity for differentiating into multiple lineages, human ASCs show potential characteristics for allogenic stem cell applications due to low immunogenicity and immunosuppressivity (Patrikoski et al., 2014).

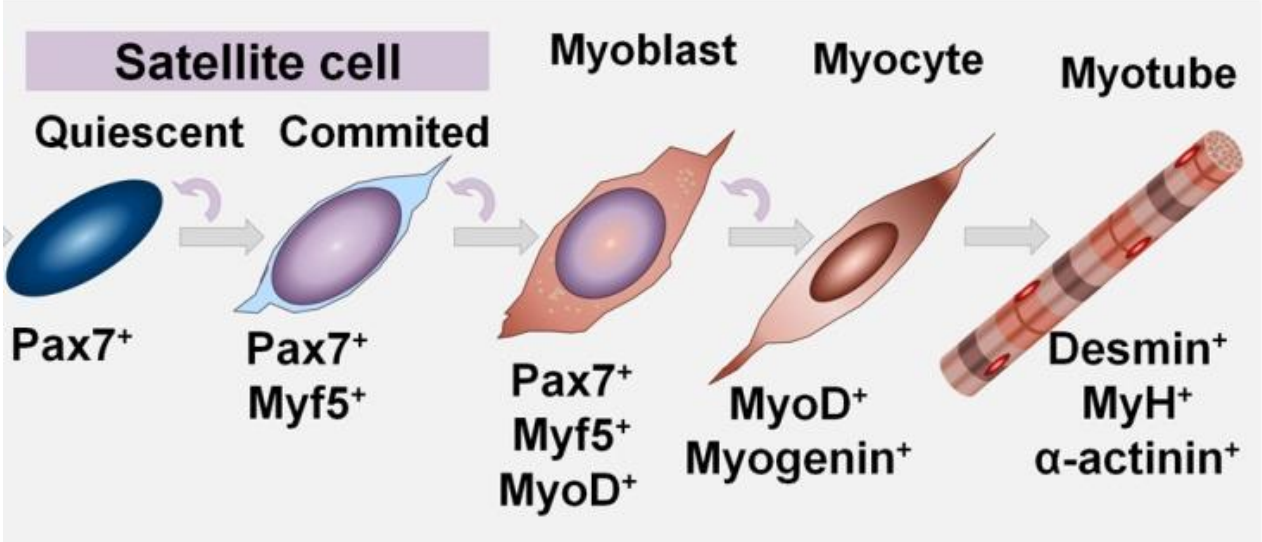

Figure 1. *Myogenic cell characterization. Myogenic cell lineage is identifiable in each state of differentiation based on the expressed myogenic markers. Cropped image from Zouraq, Stölting & Eberli, 2013.*

The myogenic potential of human MSCs in myogenic cocultures seizes to be fully characterized, and requires more research, until their full potential in skeletal tissue engineering can be understood. A study by Dugan, Cartmell and Cough indicated that coculturing with myoblasts might improve the desired mesenchymal stem cell differentiation and their fusion into myotubes (Dugan et al., 2014). Beier et al. indicated similar results with their coculture study with MSCs and rat myoblasts (Beier et al., 2011). A study by Schulze et al. strongly indicates that adult stem cells are unable to autonomously differentiate into a fully mature striated muscle, though they are described to potentially fuse with an existing myotube (Schulze et al., 2005). Di Rocco et al. further suggest that mesenchymal stem cells require contact with myogenic cells for them to acquire skeletal muscle phenotypes (Di Rocco et al., 2006). Their study also promoted the use of a differentiation medium in

the MSC expansion phase, in which the growth medium of the MSC cultures was changed to a specific differentiation medium (in a process briefly referred to as “priming” the cells).

According to the review by Truskey, Vandenburgh et al. created the first *in vitro* myobundles consisting of multinucleated myotubes (Vandenburgh et al., 1999, Truskey, 2018). As referred to in the previous chapters, engineered skeletal muscle models have been created either in 3D or with mesenchymal stem cells. However, the publications on creating 3D skeletal muscle models with mesenchymal stem cells, or optimizing the induction of MSCs’ myogenic potential, are few in number (Burdzińska et al., 2008, Di Rocco et al., 2006, Witt et al., 2017). Fibrin is one of the most suitable hydrogels for the means of engineered myobundle (EMB) formation, as it promotes the maturation of myotubes and is resilient under contractile forces (Hinds et al., 2011). EMBs are aligned through traction forces, which result from fibrin condensing, as the end of the EMBs are fixed (Madden et al., 2015).

This study utilizes and optimizes two existing indirect (or secondary) immunofluorescence protocols; immunocytochemistry (briefly ICC) for 3D samples and immunohistochemistry (briefly IHC) protocol for cryohistoslices. To evaluate the maturity of muscle structures, myosin heavy chain (referred to as MYH7) staining was used as a late myogenic marker (Gang et al., 2004). Other option for myogenic marker was desmin, described an early myogenic marker (Jalali Tehrani et al., 2014). DAPI (or 4′,6-diamidino-2-phenylindole, to be precise) was used to stain all the nuclei, and human nuclei were stained to distinguish the human and C2C12 mouse nuclei. Phalloidin staining actin was included later, to line the cell structures more appropriately.

Classical light microscopy techniques enable the imaging of thin samples, and in this study, the estimation of the living EMB thickness with the help of a scale bar. Diffraction limits the resolution in using wavelengths of visible light to 0.2 micrometers (µm). Visualizing cells and cytoskeletal elements in a greater resolution and in three dimensions require an imaging technique, that focuses on a certain plane in the specimen while rejecting the signal coming from planes above and under the focus point. Confocal microscopy focuses illuminated light (usually laser) on certain positions along the Z-axis. In laser confocal microscope, the pinhole aperture is placed at a confocal position with the laser illuminating pinhole (hence the name), so only the light focused on a specific XYZ-position in the sample is detected. (Alberts et al., 2015) To capture different stains and the corresponding cell structures in multiple channels using fluorescence microscopy, Zeiss confocal laser scanning microscopes (LSM) 780 and 800 were used. Image quality can then be enhanced using deconvolution, which utilizes point spread functions to reverse optical distortion.

To the best of my knowledge, the human ASCs’ ability to fuse with C2C12 cells into multinucleated myotubes has not been evaluated in 3D before. Based on the literature referred to in the previous

chapters, it is hypothesized that a formation of hybrid myotubes between these cell types is possible. Therefore, the goal of this study is to evaluate ability of human ASCs and C2C12 coculture EMBs to form fusion myotubes, and to optimize staining protocols and confocal imaging to reliably detect quantifying and fusion. Evaluation will include the determination of the fusion ratio, or fusion index. The fusion index describes the amount on nuclei inside multinucleated myotubes compared to the total amount of nuclei (Bajaj et al., 2011). Furthermore, this study aims towards the determination of the ASC percentage in the hybrid myotube nuclei.

2. MATERIALS AND METHODS

2.1 Materials

ASC passage 1 was acquired from an adult female donor, from the subcutaneous fat of the lower abdomen. Commercial C2C12 mouse C3H muscle myoblast cell line was supplied by European Collection of Authenticated Cell Cultures (briefly ECACC, catalog number 91031101).

Horse Serum (HS), Triton X-100, Bovine Serum Albumin (BSA), fibrinogen, 4′,6-diamidino-2-phenylindole (DAPI), Thrombin and human Anti-Nuclei primary antibody (MAB1281) were purchased from Sigma-Aldrich. 10 % Fetal Bovine Serum (FBS), alfa Minimum Essential Medium (αMEM), secondary antibodies, Trypan Blue, Invitrogen ProLong mountants (with and without DAPI) and primary antibodies Desmin (PA5-19063) and MYH7 (222-1-AP) were purchased from ThermoFisher Scientific. Tissue-Tek O.C.T. Compound embedding medium was purchased from Sakura. Aprotinin was from Abcam. Phalloidin was from ATTO-TEC. Vectashield Antifade Mounting Medium was purchased from Vector Laboratories. DPBS used was purchased from Lonza. Immersol immersion oil was purchased from Carl Zeiss Microscopy. Penicillin streptomycin (P/S) was purchased from BioWhittaker. Tryple was purchased from Life Technologies.

2.2 ASC isolation, culturing, and flow cytometry

The ASC isolation, expanding and flow cytometry analysis were performed previously in the Adult Stem Cell research group. The isolation protocol of the ASCs used has been described on previous publications (Lindroos et al., 2009, Gimble, Guilak, 2003, Hyväri et al., 2020). To summarize, the obtained adipose tissue was digested, centrifuged, and filtered to separate stem cells from the sample. The adipose tissue was attained with written informed consent in accordance with the Regional

Ethics Committee of the Expert Responsibility are of Tampere University Hospital, under the ethical approval R15161.

Fluorescence-activated Cell Sorting (FACS) was conducted on the ASC cell line to indicate that it meets the criteria of mesenchymal stem cell definition (Dominici et al., 2006). To evaluate the immunophenotype and previously reported cluster of differentiation (CD) markers for multipotency, the following markers were tested: CD11a/b, CD14, CD19, CD34, CD45, CD54, CD73, CD90, CD105, and HLA-DR.

2.3 Cell Expansion

The cells were expanded separately in 10% FBS in αMEM in T175 flasks. The ASCs were defrosted and plated at cell density of 4000 cells per cm2, expanded for 12 days and passaged once. The cells were counted to determine the cell concentrations the next passage. Medium was changed and the cells were microscoped twice a week. C2C12 cells were defrosted, suspended in prewarmed 10 % FBS αMEM and plated at cell density of 1300 cells per cm2 and expanded for 3 days up to 70% of confluency. Monitoring the C2C12 confluence is important to retreat from inducing differentiation in the expansion phase. The cells were microscoped and medium was changed twice a week. Every passage protocol was performed by detaching the cells with Tryple and by centrifuging the cells for 5 min at 1000 RPM to form a cell pellet.

Priming medium was added on some of the ASC cultures; 5 % fetal bovine serum (FBS), 5 % horse serum (HS), 10 µg/ml insulin, 1% P/S (Penicillin-Streptomycin) in αMEM (alfa Minimum Essential Medium, Gibco). Priming medium was added two days prior to the EMB fabrication, where the cocultures were simultaneously formed. The cell concentration was set on 15 million cell per ml (the cells being counted with Bürker chamber, stained with Trypan Blue).

2.4 EMB formation

For the EMB formation, a mixture of fibrinogen and thrombin was used to form fibrin following the protocol on Khodabukus et al. with some modifications (Khodabukus et al., 2019). Experimental groups consist of C2C12 and primed coculture setups. Non-primed experimental group was discarded from this study due to EMB breakage before fixing. For cocultures, ASC- and C2C12 cell lines were mixed in 1:1 ratio.

To sterilize the molds, the PVP coated PDMS molds and frames with Velcro were treated with 70% ethanol for 10 min, followed by 1 hour UV treatment during evaporation. Velcro was previously glued to the frames using aquarium glue. The fibrin suspension containing the cells was made by pipetting the reagents to an eppendorf tube on ice, in the following order: the room temperature (briefly RT) cell suspension, 0,5 molar (M) calcium chloride ($CaCl_2$), 10 % FBS αMEM, 100 units

per milliliter (U/ml) Thrombin and 20 mg/ml Fibrinogen. The suspension was quickly pipetted to the PDMS molds, and the Velcro-frame was placed on the mold with the hooked side set to face the channel and imbedded into the suspension. 10 % FBS αMEM with 40 µm/ml aprotinin was added. The EMBs were moved to a 37 ◦C incubator. The medium (10 % FBS αMEM with 40 µm/ml aprotinin) was changed every two days. The EMB cultures were fixed to 7-day and 14-day timepoints.

2.5 Immunocytochemistry

An existing immunocytochemistry was used and modified to suit the needs of this study. The protocol was optimized throughout the study. Prior to fixing, the EMBs were imaged with light microscope for thickness measurements with the help of a scale bar. The EMBs were fixed in 4% PFA in 1xPBS for one hour at RT, in a laminar hood. Two 10 min washes in 1xPBS followed. The EMB structures, for which the immunocytochemistry was tested on, were from a prior experiment iteration.

The frames were detached and the EMBs were cut and placed on a 96-well plate after fixing. Triton X-100 concentrations from 0,2-0,5 % were tested, settling on the 0,5 % concentration. The samples were incubated in 0,5 % Triton X-100 in 5% BSA in 1xPBS for 2 h at RT, for blocking and permeabilization. 5 min wash in the 5% BSA in 1xPBS (later referred to as the “blocking solution”) followed.

Primary antibodies were diluted in blocking solution and centrifuged for 3 min at 13 000 rounds per minute (RPM) for solution homogenization. For desmin, the ratio was set on 1:200. MYH7 concentrations of 1:100 and 1:200 were tested, as for human nuclei ratios of 1:50 and 1:100 were applied, settling for the latter ones in both cases. The samples were incubated in primary antibody solutions overnight at +4 ◦C (in agitation). One quick wash and three 1,5 h washes at RT in agitation were executed in blocking solution.

From this point onwards, the light-sensitive solutions and stained samples were treated protected from light. Secondary antibodies were diluted in blocking solution in a ratio of 1:400 and homogenized similarly to primary antibody solutions. Samples were incubated in secondary antibody solutions for 45 min at RT in agitation. One quick wash and a 30 min wash in 1xPBS at RT followed (again in agitation), and the latter wash was prolonged to 1 h.

DAPI was diluted in 1xPBS in 1:1500 ratio and incubated for 30 min in agitation. One quick wash and three long washes in 1xPBS followed, such as two 30 min washes at RT and one overnight wash at +4 ◦C in agitation.

2.6 Immunohistochemistry

The EMSs from cell culture experiment described in chapters **2.3** and **2.4** were used, when starting the staining experiments on an immunohistochemistry protocol. Based on literature, cryohistoslices and an existing immunohistochemistry protocol were applied. The EMBs were cut from the frames and Velcro. The EMBs were fixed as described in chapter *2.3 Immunocytochemistry.* PFA solution was washed twice with 1 x PBS. O.C.T. (Tissue-Tek) was added for the samples overnight in +4 °C. The samples were quickly frozen by dipping a decanter filled with 2-methylbutane in liquid nitrogen and lowering the sample in its O.C.T. -containing mold into the decanter. After freezing, the samples were stored in -80 °C.

Cryoslice thicknesses tested were 10-40 micrometers thick. The EMBs were cut as longitudinal slices, trying to fit the whole length of the structure on each slice. After one test performing cryoslice staining through droplets, rest of the samples were stained by inserting the SuperFrost-glasses to a custom rack setup from an automatic staining device.

Permeabilization was first treated as a separate step (15 min at RT in 0,2% Triton X-100 in 5% BSA in PBS) from blocking, which followed after as 5% BSA in PBS for 45 min at RT. Through optimization, Triton-concentration was raised and permeabilization and blocking were combined into a step consisting of 0,5% Triton X-100 in 5% BSA in PBS for 1 h at RT. Two quick washes in blocking solution followed.

Primary antibodies were diluted in blocking solution and homogenized as described earlier. The samples were incubated in primaries for 1 h at RT. Four 3 min washes in blocking solution followed.

From this point onwards, the light-sensitive solutions and stained samples were treated protected from light with aluminum foil. Secondary antibodies were diluted in blocking solution and homogenized as described earlier. Ratio for all secondary antibodies was first at 1:400, and later it was set to 1:200. Samples were incubated in secondary antibody solutions for 45 min at RT in dark. Two 3 min long washes in PBS followed.

DAPI was diluted in 1xPBS in 1:2000 ratio and incubated for 5 min. Phalloidin was added to this step in 1:400 ratio for staining the actin filaments of the cells. Since the addition, incubation time in the DAPI-phalloidin dilution was raised to 15 min.

2.7 Imaging

The samples were first mounted in Vectashield including DAPI. Later Vectashield was changed to Prolong with DAPI, which was again replaced with its counterpart not including DAPI.

The stained samples were imaged with the Zeiss 800 confocal fluorescence microscope, later moving onto the LSM780. Three separate channels were used until the addition of phalloidin. Objectives used were 10x magnification air objective and 25x magnification multi-immersion objective with Immersol immersion oil.

Though the 3D reconstruction itself is outside the scope of this thesis, all the factors were optimized for image reconstruction purposes. Hyugens Scientific Volume Imaging (SVI) software was used for deconvolution of the images. Deconvolution set certain demands on the imaging parameters on the Zeiss LSM800/LSM780 during the imaging.

The images were enhanced using ImageJ and open-source image processing package Fiji, as well as the Hyugens SVI software.

3. RESULTS

3.1 Optimizing staining & imaging

To enable possible detection of myotube structures, the objective used should provide a comprehensive overview of the sample, as well as depicting a high-definition image of the structures of interest. The 25x multi-immersion objective was found to provide information on an appropriate scale for this study, contrary to the 10x air objective. The change of mountant from liquid Vectashield to hardening Prolong made the imaging and storing the samples easier. The refractive index on Prolong is similar to those of the immersion oil and microscopy glass used.

After raising the Triton X-100 concentration in immunocytochemistry phase to 0,5 %, we detected the first successful HuNu staining in our experiments. As seen in *Figure 2.,* HuNu (red) and DAPI (blue) overlap, staining the same nuclei. With the help of a scale bar set in ImageJ, nuclei width can be estimated around 10 µm. One should note that the amount of background is high and should be optimized further.

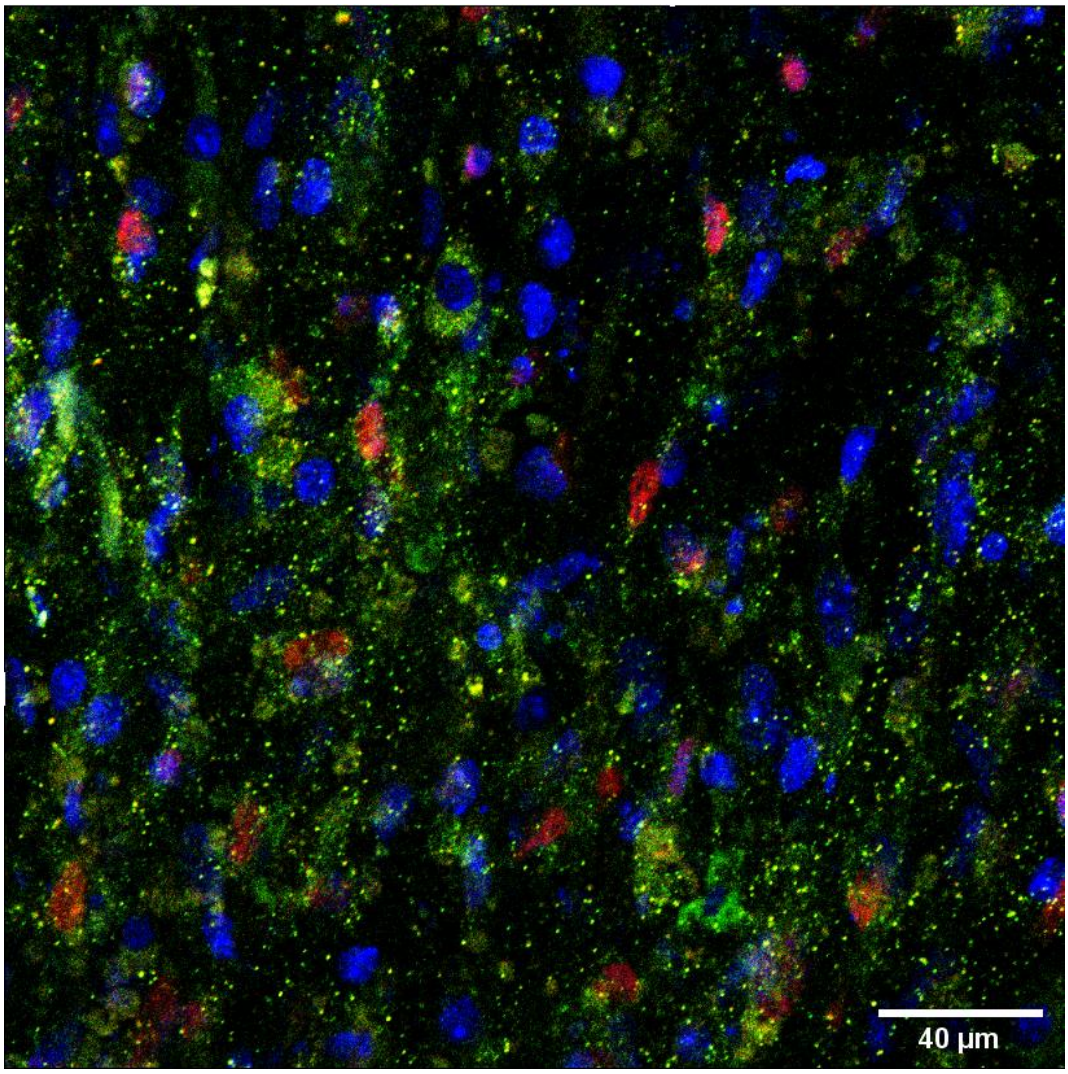

Figure 2. *First successful human nuclei staining iteration. Taken on LSM800. ICC on a 3D sample. Color representation: red; HuNu, blue; DAPI, green; desmin.*

Figure 3. displays 14-day timepoint primed cocultures, in which desmin in displayed on the left and MYH7 on the right, both in green. In these staining iterations, MYH7 appeared to line the cells more appropriately than desmin, while working as a myogenic marker. Using the scale bar, the nuclei in both pictures was estimated to again be approximately 10 µm and their morphology appears to be quite round. The cells appear to be oriented along a certain axis.

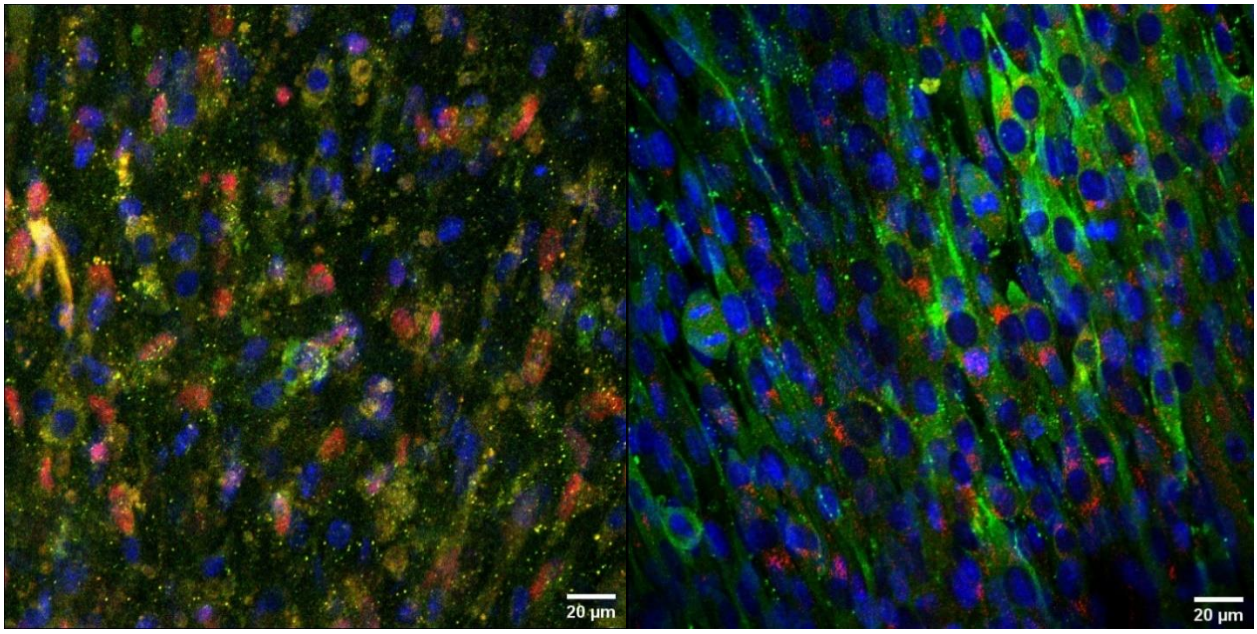

Figure 3. *14-day timepoint primed coculture displaying desmin (left) and MYH7 (right). Taken on LSM800. ICC on a 3D sample. Color representation: red; HuNu, blue; DAPI, green; desmin/MYH7.*

7-day and 14-day timepoints of primed cocultures are displayed in *Figure 4.* Nuclei appear to be more stretched compared to *Figure 3.* and appear to be approximately 6-8 µm wide. Cells appear distinctively oriented along a certain axis.

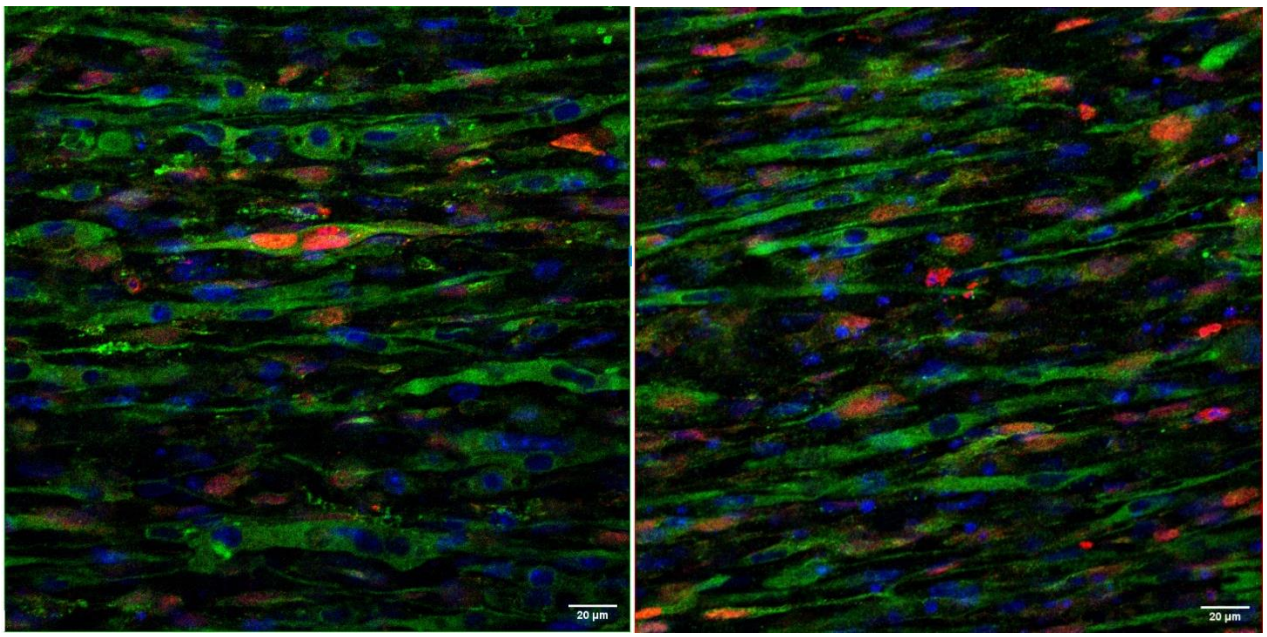

Figure 4. *Image displaying the 7-day and 14-day primed cocultures. 3D-samples imaged on LSM800 with 25x multi-immersion objective with immersion oil. Image enhanced with ImageJ. ICC on a 3D sample.*

ICC stained samples presented in *Figures 2-4* displayed the structures on the peripheries of the samples. Yet, the ICC protocol was unable to stain the samples thoroughly, leaving a large proportion of the sample unstained and useless. Therefore, the staining process was changed to immunohistochemistry protocol (initially intended for 2D samples).

Phalloidin was found useful in staining the actin and therefore lining the outer parts of cell cytoskeletons and possibly enabling more reliable detection of DAPI localization. *Figure 5.* shows a deconvoluted Hyugens SVI maximum intensity projection (MIP) rendering of red phalloidin lining the actin cytoskeleton of the cells on 14-day C2C12 and primed coculture samples. MIP rendering makes visual localization of nuclei (stained with DAPI in this figure) easier. The nuclei appear, again, to be around 6-8 µm in width. Both round and more elongated morphologies appear to be present. Cells appear to be clearly oriented. Some multinucleation appears, though the myotube outlines appear to align the nuclei, making them approximately no more than 10 µm thick in the C2C12 sample. The C2C12 sample appears to be less crowded by nuclei than the coculture. The myotube thickness in the C2C12 sample appears to be larger than in the coculture. The channel depicting DAPI appears to have a high amount of background noise, especially in the coculture.

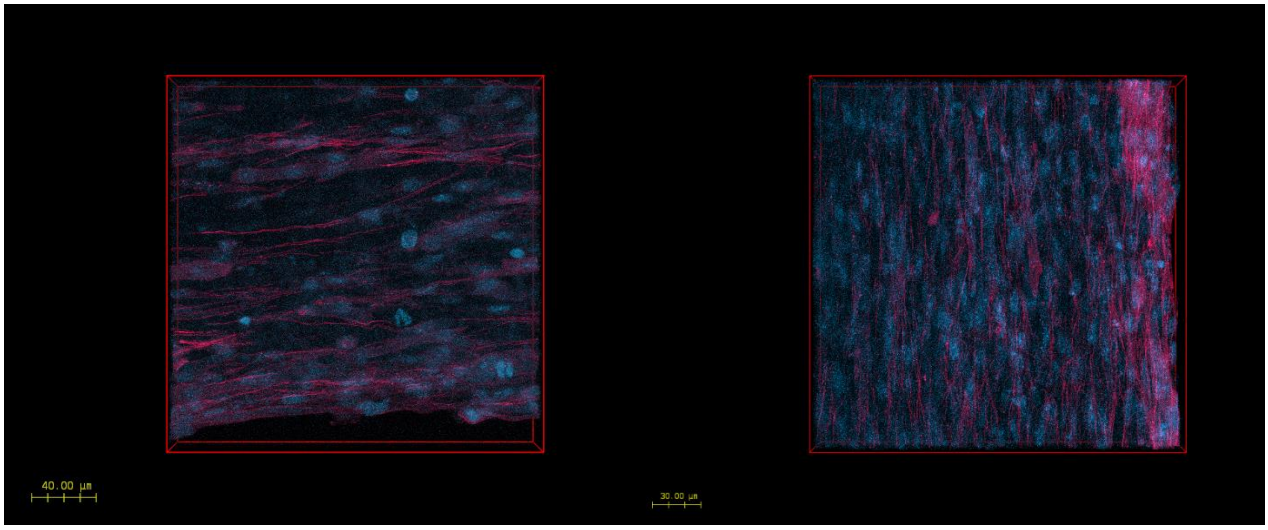

Figure 5. *MIP rendering of phalloidin lining the cells in 14-day C2C12 and primed cocultures. Taken on LSM780 with 25x multi-immersion objective with immersion oil. IHC on a 30 µm cryoslice. Deconvoluted and enhanced with Hyugens SVI. Color representation: blue; DAPI, red; phalloidin.*

Figure 6. displays a similar MIP rendering of a 14-day primed coculture. The nuclei width is approximately 6-8 µm, although their morphology appears strongly elongated compared to the previous pictures. Some multinucleation appears, and the myotube thickness seems to be mostly aligned with the nuclei width, though some thicker formation might also appear. Cells appear, again, to be clearly oriented along a certain direction. Prolong mountant containing DAPI was changed to one,

where DAPI is not included, and based on *Figure 6.* the background noise from the DAPI-depicting channel seems to be reduced.

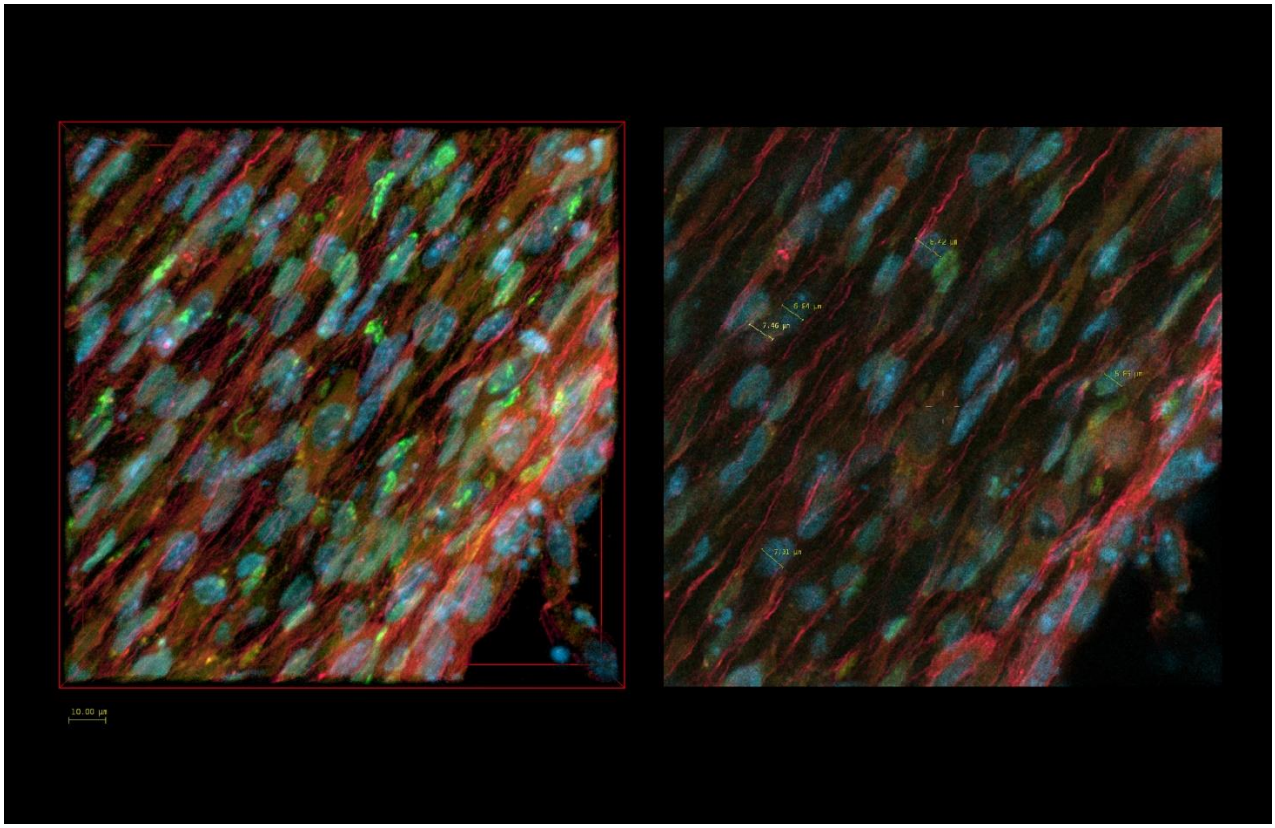

***Figure 6**. A MIP rendering (left) and a Hyugens slice view (right) of a 14-day primed coculture. Taken on LSM780 with 25x multi-immersion objective with immersion oil. IHC on a 30 µm cryoslice. Deconvoluted and enhanced with Hyugens SVI. Color representation: green; HuNu, blue; DAPI, red; phalloidin, orange; MYH7.*

3.2 Optimizing cryoslices

Cryoslice thicknesses of 10, 20, 30 and 40 micrometers (µm) were tested. 20 and 30 µm were found to be the most suitable for our purposes. Slices with the thickness of 40 µm started to show signs of detachments when moved onto the SuperFrost-glass, although the ones that stayed sustained the staining process as well as the thinner slices. Slices with the thickness of 10 µm stuck to the SuperFrost well, but their thickness is lower than the estimated thickness of the muscle cells. Therefore 10 µm slices could not display intact muscle cells and therefore myotubes. Slices with the thickness of 20 and 30 µm seemed to be able to include intact myotube structures, and the cells did not appear to be broken (as seen in *Figure 5.,* demonstrated on a 30 µm thick sample).

3.3 Enhancing images

Hyugens SVI software was used for image deconvolution. As displayed in *Figure 7.*, the deconvolution process seems to reduce the background noise and enhance resolution.

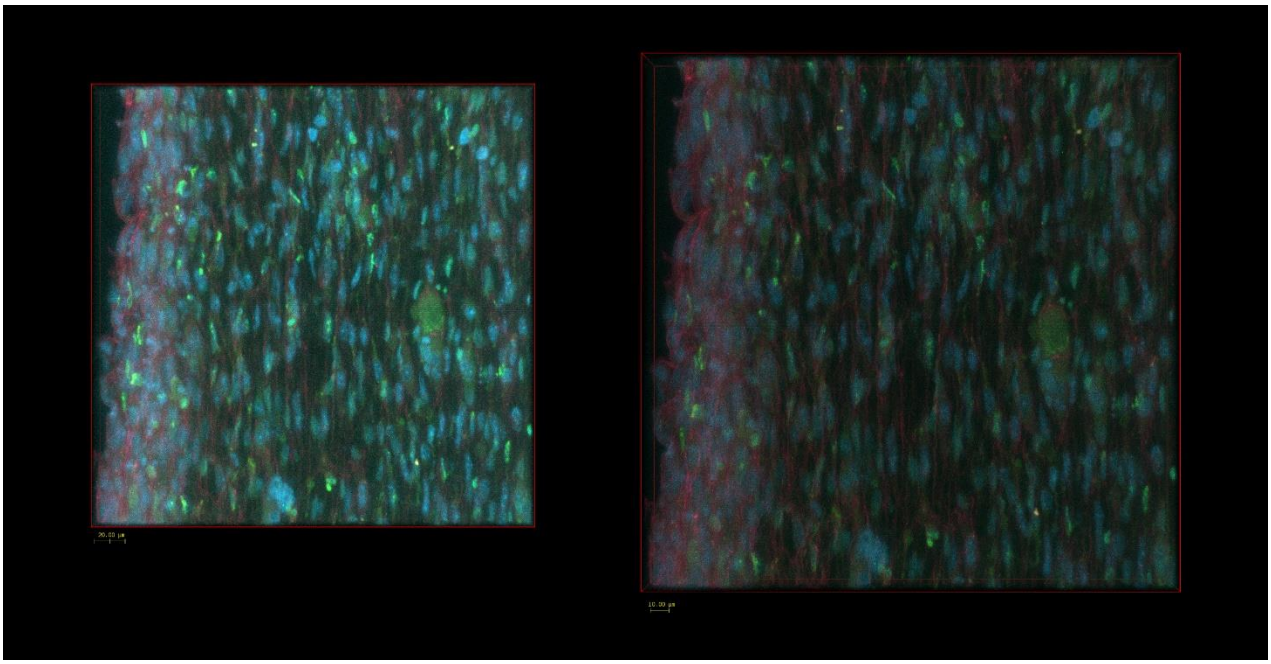

Figure 7. *XY-view on the sample before (left) and after (right) deconvolution. 14-day primed coculture. Taken on LSM780 with 25x multi-immersion objective with immersion oil. IHC on a 30 µm cryoslice. Deconvoluted and enhanced with Hyugens SVI. Color representation: green; HuNu, blue; DAPI, red; phalloidin, orange; MYH7.*

Figure 8. demonstrates the effect of deconvolution to the Z-axis resolution. The distribution of the signal appears to be distributed to a narrower scale along the Z-axis, which suggests improvement in resolution.

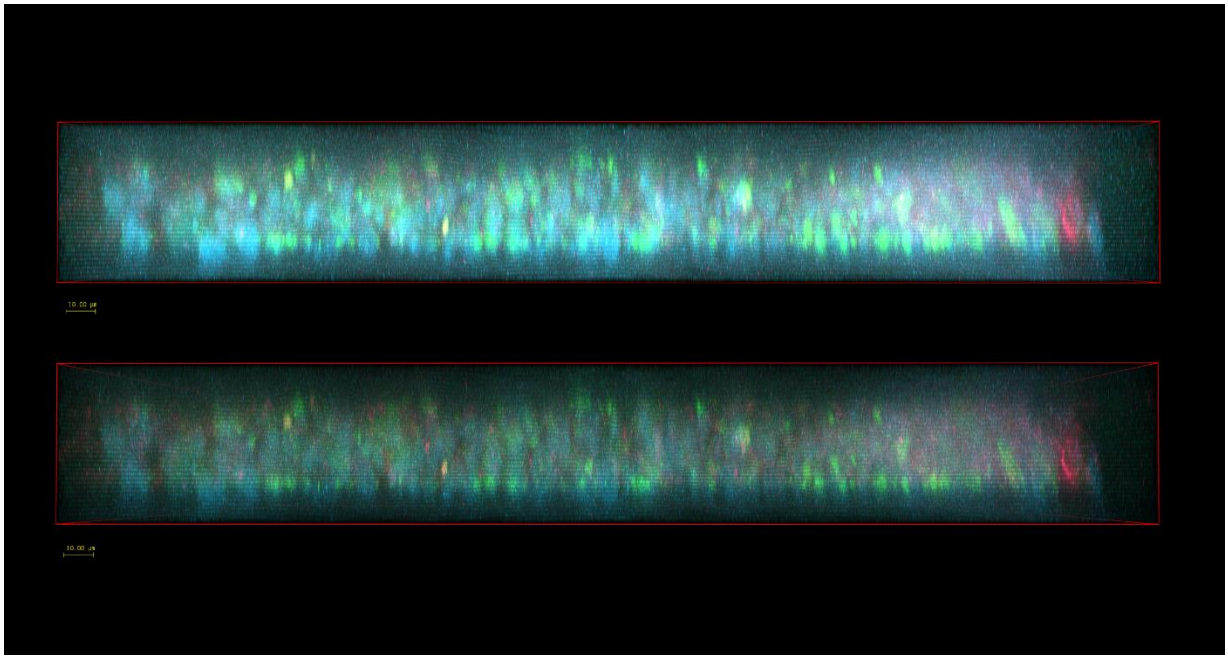

Figure 8. *Z-axis view on the sample before (upper) and after (lower) deconvolution. 14-day primed coculture. Taken on LSM780 with 25x multi-immersion objective with immersion oil. IHC on a 30 µm cryoslice. Deconvoluted and enhanced with Hyugens SVI. Color representation: green; HuNu, blue; DAPI, red; phalloidin, orange; MYH7.*

4. DISCUSSION

Reliably localizing the nuclei inside the myotube structures became increasingly more credible, as phalloidin was taken into the staining protocol for lining the cell structures. As the resolution was enhanced through iterations and image editing, the approximate nuclei size appeared to increasingly correspond to the values described in literature. Phalloidin enables approximations of the myotube thicknesses, which seemed to mostly be aligned with the nuclei inside them. *Figures 3-8.* clearly show the sell structures oriented along a certain axis, presumably defined by the direction of the mechanical strain. When examining the images captured, some possible ASC fusion was visually detected, though no colocalization measurements were made. *Figure 9.* acts as a 2D sample reference image, demonstrating how close together distinct nuclei might be packed. At this point, this study suggests that it is not possible to distinguish whether a single fragmented and/or elongated nuclei or two distinctive nuclei are observed in the confocal images. Using greater magnification might increase the distinguishability. Staining nuclear lamins might also facilitate nuclei detection by lining the nuclear envelope.

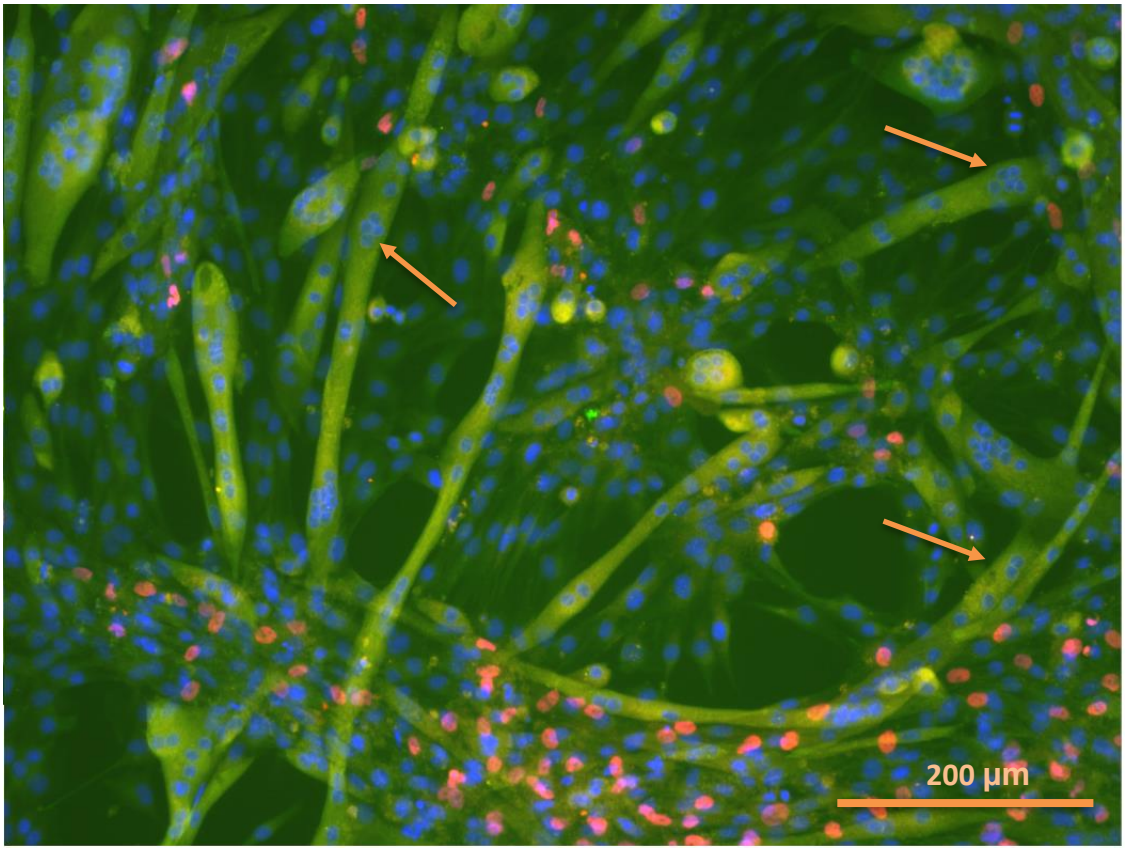

Figure 9. *Reference image for 2D samples of a 8-day primed coculture. Taken on Olympus IX51 with 10x air objective. ICC for 2D samples. Enhanced in ImageJ. Color representation: green; MYH7, blue; DAPI, red; HuNu. (Original image captured by Björninen, M.)*

As stated in the introduction, fusion ratio describes the amount on nuclei inside multinucleated myotubes compared to the total amount of nuclei (Bajaj et al., 2011). Some studies measure the fusion ratio (or fusion index) in myofiber area (McColl et al., 2016). Neither of these ratio determination approaches provide direct information about the nuclei origins themselves, when considering a coculture experiment, but the fusion ratio determination described by Bajaj et al. suits the needs of this study better. In addition to the independence from the nuclei amount itself, the myofiber area -measuring approach would presumably demand the cryoslices to be cross sectioned, contrary to the longitudinal slices used in this study.

Many EMB studies referenced to in this thesis provide quantitative Western blot-results of protein expression supporting the immunostaining result images. In this case, this could mean quantification of the myogenic differentiation markers (Hinds et al., 2011). After the staining and imaging protocols are optimized, quantifying the potential expression of myogenic differentiation markers would support the conclusions drawn from the fluorescence images. Measuring the myogenic markers on set timepoints could help to characterize whether ASCs follow the myogenic differentiation lineage phases.

Background noise reduction through deconvolution and increased wash volumes in staining contributed to the overall resolution and therefore to the visual and qualitative evaluation of the nuclei localization. It is also suggested that the reduced background will improve quantitative analysis, for example by easing the defining the threshold for cell outlines (which is usually required in digital image analysis steps). Changing the ICC protocol to IHC makes it possible to utilize most of the 3D EMB sample slices horizontally, while the slices are still thick enough to contain complete myotube structures.

Deciding the magnification used for capturing parallel images considers a couple of factors. Imaging with 10x air objective enables us to capture a larger frame of the sample, but 25x multi-immersion objective with immersion oil provides sharper images, with a better chance for useful 3D reconstruction and rendering properties. The latter might be more suitable in capturing images for 3D reconstruction on Imaris 9.5. The overlapping nature and length of the myotubes complicates the imaging of a single myotube. One of the difficulties faced in this study underlines the importance of nuclei localization in three dimensions; LSM800 had to be changed to LSM780 midst the experiments, as the DAPI localization failed to succeed, therefore precluding 3D colocalization analysis of human and mouse nuclei.

Using immunohistochemistry on the myobundle cryoslices creates more optimizable aspects, beyond the scope of this thesis. One thing to consider is, what would be the maximum cryoslice thickness providing viable information, where the stains could still penetrate the sample. This was not tested in this study, as the stated in the chapter **3.2**. Staining the 3D samples prior to cryoslice experiments and analyzing those image stacks could have provided some insight on this, but the apparent DAPI penetration depth seen is unreliable due to imaging difficulties on LSM800. As described by Khodabukus et al., the lack of vascularization creates certain limits for the myotube size (Khodabukus et al., 2019). One should consider, if the non-vascularized setup creates unwanted divergency between the cryoslices taken from the EMB periphery, contrary to the samples taken from the middle of the structure. This applies to the ICC treated 3D samples as well – if the ICC enables the visualization of only the outer layers of the sample, divergency among different sample depths might occur.

Using Prolong not containing DAPI seemed to better the results by possibly reducing DAPI channel background noise. Compared to air, Prolong's refractive index resembles those of glass and immersion oil used. Because of this, the dispersion of light and consequent chromatic aberration is smaller and focusing on the specimen enhances (Ford, Freedman & Young, 2012), increasing the overall image quality. Using larger wash volumes in the last immunohistostaining iteration seemed to contribute to background reduction. Growing the secondary antibody concentration also seemed to enhance the overall resolution.

5. CONCLUSIONS

This study aimed to improve the reliable detection of ASC nuclei localization inside the myotubes and to advance towards fusion ratio determination. The latter is attempted to achieve by optimizing the sample preparation, staining, and imaging protocols for 3D engineered skeletal muscle bundles.

Through multiple optimizing iterations of the staining protocols and confocal imaging, both the immunocytochemistry and immunohistochemistry protocols were further optimized. Raising the Triton X concentration seems to improve the penetration of human nuclei stain into the ASC nuclei. Increasing wash volumes and secondary antibody concentrations seemed to improve the image quality and reduce background. Using a mountant not containing DAPI seemed to reduce background noise on the respective channel when imaged. Using a curing mountant also bypasses the need for acrylic resins used in setting the sample between the microscopy slide and cover glass, which makes the mounted sample easier and cleaner to handle.

MYH7 was detected to be an appropriate marker for both depicting the myoblast structure and acting a late muscle marker. Though it is reported to express in slow fenotype, it appeared to stain cells depicting myotube morphology in both timepoints of this study.

The optimized immunohistochemistry protocol was suggested as the more prominent staining approach, when interests are utilizing majority of the sample and depicting intact myotubes. The optimal cryoslice thickness at this phase of the larger-scale study was estimated to be around 20 to 30 µm, balancing between capturing complete longitudinal muscle cells and being suitably thin for IHC staining protocol and staining rack.

Deconvolution through Hyugens SVI software enabled the enhancement of our picture stacks without the drawbacks of increased photon load on the samples. Deconvolution also seems to serve as a valuable pre-step for 3D reconstruction, as it considerably betters the resolution when visualizing sample contents along the Z-axis, as demonstrated in *Figure 7.*

LIITE: OPTIMIZED IMMUNOCYTOCHEMISTRY PROTOCOL

3D EMB IMMUNOSTAINING PROTOCOL - OPTIMIZED

[ ] FIXING: 4% PFA in 1x PBS for 1h at RT (depends on gel thickness)

[ ] DETACHING THE FRAME: Cut EMBs into 2 pieces and move them into 96-well plate

[ ] WASHING: 2 washes in 1x PBS for 10 min (or longer) each

Samples can be left in the second wash for later use.

[ ] BLOCKING: 0.5% Triton-X in 5% BSA in 1xPBS for 2h at RT

[ ] WASHING: 5% BSA in 1x PBS for 5 min

[ ] MIXTURE OF PRIMARIES: diluted in the same solution as for blocking

Primary antibody	V, µl	dilution	origin
Desmin		1:200	
HuNu		1:100	
MYH7		1:200	

- Centrifuged 3 min 13 000 rpm to homogenize the solution
- Incubation overnight at +4^{0}C

[ ] WASHING: 5% BSA in 1x PBS: 1x quick wash + 3 washes for 1,5 h each

[ ] MIXTURE OF SECONDARIES in 5% BSA in PBS,

Secondary antibody	V, µl	dilution	origin
		1:400	
		1:400	

- Centrifuged 3 min 13 000 rpm to homogenize the solution
- Incubation 45 min at RT

[ ] WASHING: in 1x PBS, 1x quick wash + 1x 1h wash at RT

[ ] DAPI (AND PHALLOIDIN): 1:1500 DAPI (and 1µg/ml TRITC-Phalloidin (optional))

- Incubation 30 min at RT

[ ] WASHING: in PBS, 1x quick wash + 3x long washes, (e.g. 30min, 1h, overnight)

[ ] STORE: +4^{0}C protected from light, mounted in Prolong Gold (not containing DAPI)

LIITE: OPTIMIZED IMMUNOHISTOCHEMISTRY PROTOCOL

2D EMB IMMUNOSTAINING PROTOCOL - OPTIMIZED

[ ] **FIXING**: 4% PFA in 1x PBS for 1h at RT

[ ] **WASHING**: 2 washes in 1x PBS (first PBS waste into PFA-waste)

Samples can be left in the second wash for later use, in +4^{0}C.

[ ] **BLOCKING & PERMEABILIZATION**: 0,5% Triton-X in 5% BSA in 1xPBS for 1h at RT

[ ] **WASHING**: 2 quick washes in 5% BSA in 1x PBS (= blocking solution)

[ ] **MIXTURE OF PRIMARIES**: diluted in the same solution as for blocking

Primary antibody	V, µl	dilution	origin
		1:100	
		1:100	

- Centrifuged 3 min 13 000 rpm to homogenize the solution
- Incubation 1 h at RT

[ ] **WASHING**: 4x with 5% BSA in 1x PBS, 3 min in every round

[ ] **MIXTURE OF SECONDARIES** (in dark, from this point onwards)

- Diluten iin 5% BSA in PBS,

Secondary antibody	V, µl	dilution	origin
		1:200	
		1:200	

- Centrifuged 3 min 13 000 rpm to homogenize the solution
- Incubation 45 min at RT

[ ] **WASHING**: 2x with 1x PBS, incubating 3 min in every round

[ ] **DAPI (AND PHALLOIDIN)**: 1:2000 DAPI and 1:400 Phalloidin diluted in PBS (work in laminar hood)

- Incubation 15 min at RT (in laminar)

[ ] **WASHING**: 1x in 1x PBS (first waste into Phalloidin-waste)

[ ] **STORE:** +4^{0}C protected from light, mounted in Prolong Gold (not containing DAPI)

[ ] **STORE:** +4^{0}C protected from light, mounted in Prolong Gold (not containing DAPI)

REFERENCES

Alberts, B., Johnson, A., Lewis, J., et al. 2015, *Molecular Biology of the Cell,* Sixth edition, Garland Science, Taylor & Francis Group, New York, NY.

Bajaj, P., Reddy, B., Millet, L., et al. 2011, "Patterning the differentiation of C2C12 skeletal myoblasts", *Integrative biology : quantitative biosciences from nano to macro,* vol. 3, no. 9, pp. 897-909.

Battula, V.L., Bareiss, P.M., Treml, S., et al. 2007, "Human placenta and bone marrow derived MSC cultured in serum-free, b-FGF-containing medium express cell surface frizzled-9 and SSEA-4 and give rise to multilineage differentiation", *Differentiation; research in biological diversity,* vol. 75, no. 4, pp. 279-291.

Beier, J.P., Bitto, F.F., Lange, C., et al. 2011, "Myogenic differentiation of mesenchymal stem cells co-cultured with primary myoblasts", *Cell biology international,* vol. 35, no. 4, pp. 397-406.

Burdzińska, A., Gala, K., Paczek, L. 2008, "Myogenic stem cells", *Folia Histochemica Et Cytobiologica,* vol. 46, no. 4, pp. 401-412.

Di Rocco, G., Iachininoto, M.G., Tritarelli, A, et al. 2006, "Myogenic potential of adipose-tissue-derived cells", *Journal of Cell Science,* vol. 119, no. 14, pp. 2945-2952.

Dominici, M., Le Blanc, K., Mueller, I., et al. 2006, "Minimal criteria for defining multipotent mesenchymal stromal cells. The International Society for Cellular Therapy position statement", *Cytotherapy,* vol. 8, no. 4, pp. 315-317.

Dugan, J.M., Cartmell, S.H., Gough, J.E. 2014, "Uniaxial cyclic strain of human adipose–derived mesenchymal stem cells and C2C12 myoblasts in coculture", *Journal of tissue engineering,* vol. 5, pp. 2041731414530138.

Ford, A.L., Freedman, R.A., Young, H.D. 2012, *Sears and Zemansky's university physics: with modern physics,* 13th edition, Addison-Wesley.

Gang, E.J., Jeong, J.A., Hong, S.H., Hwang, S.H, et al. 2004, "Skeletal Myogenic Differentiation of Mesenchymal Stem Cells Isolated from Human Umbilical Cord Blood", *STEM CELLS,* vol. 22, no. 4, pp. 617-624.

Gimble, J., Guilak, F. 2003, "Adipose-derived adult stem cells: isolation, characterization, and differentiation potential", *Cytotherapy,* vol. 5, no. 5, pp. 362-369.

Hinds, S., Bian, W., Dennis, R.G., Bursac, N. 2011, "The role of extracellular matrix composition in structure and function of bioengineered skeletal muscle", *Biomaterials,* vol. 32, no. 14, pp. 3575-3583.

Huang, Y., Dennis, R.G., Larkin, L., Baar, K. 2005, "Rapid formation of functional muscle in vitro using fibrin gels", *Journal of Applied Physiology,* vol. 98, no. 2, pp. 706-713.

Hyväri, L., Vanhatupa, S., Halonen, et al. 2020, "Myocardin-Related Transcription Factor A (MRTF-A) Regulates the Balance between Adipogenesis and Osteogenesis of Human Adipose Stem Cells", *Stem Cells International,* vol. 2020.

Jalali Tehrani, H., Parivar, K., Ai, J., Kajbafzadeh, A., et al. 2014, "Effect of Dexamethasone, Insulin and EGF on the Myogenic Potential on Human Endometrial Stem Cell", *Iranian Journal of Pharmaceutical Research : IJPR,* vol. 13, no. 2, pp. 659-664.

Khodabukus, A., Madden, L., Prabhu, N.K., Koves, T.R., et al. 2019, "Electrical stimulation increases hypertrophy and metabolic flux in tissue-engineered human skeletal muscle", *Biomaterials,* vol. 198, pp. 259-269.

Kocaefe, C., Balci, D., Hayta, B.B., Can, A. 2010, "Reprogramming of human umbilical cord stromal mesenchymal stem cells for myogenic differentiation and muscle repair", *Stem cell reviews and reports,* vol. 6, no. 4, pp. 512-522.

Lindroos, B., Boucher, S., Chase, L et al. 2009, "Serum-free, xeno-free culture media maintain the proliferation rate and multipotentiality of adipose stem cells in vitro", *Cytotherapy,* vol. 11, no. 7, pp. 958-972.

Madden, L., Juhas, M., Kraus, W.E., et al. 2015, "Bioengineered human myobundles mimic clinical responses of skeletal muscle to drugs", *eLife,* vol. 4, pp. e04885.

McColl, R., Nkosi, M., Snyman, C., Niesler, C. 2016, "Analysis and quantification of in vitro myoblast fusion using the LADD Multiple Stain", *BioTechniques,* vol. 61, no. 6, pp. 323-326.

Pasut, A., Jones, A.E. & Rudnicki, M.A. 2013, "Isolation and culture of individual myofibers and their satellite cells from adult skeletal muscle", *Journal of visualized experiments : JoVE,* vol. (73):e50074. doi, no. 73, pp. e50074.

Patrikoski, M., Sivula, J., Huhtala, H., Helminen, M., et al. 2014, "Different Culture Conditions Modulate the Immunological Properties of Adipose Stem Cells", *Stem Cells Translational Medicine,* vol. 3, no. 10, pp. 1220-1230.

Rao, L., Qian, Y., Khodabukus, A., Ribar, T., Bursac, N. 2018, "Engineering human pluripotent stem cells into a functional skeletal muscle tissue", *Nature Communications,* vol. 9, no. 1, pp. 126.

Safford, K.M., Hicok, K.C., Safford, S.D., et al. 2002, "Neurogenic differentiation of murine and human adipose-derived stromal cells", *Biochemical and biophysical research communications,* vol. 294, no. 2, pp. 371-379.

Schiaffino, S., Reggiani, C. 2011, "Fiber types in mammalian skeletal muscles", *Physiological Reviews,* vol. 91, no. 4, pp. 1447-1531.

Schulze, M., Belema-Bedada, F., Technau, A., Braun, T. 2005, "Mesenchymal stem cells are recruited to striated muscle by NFAT/IL-4-mediated cell fusion", *Genes & development,* vol. 19, no. 15, pp. 1787-1798.

Stock, U.A., Vacanti, J.P. 2001, "Tissue Engineering: Current State and Prospects", *Annual Review of Medicine,* vol. 52, no. 1, pp. 443-451.

Tedesco, F.S., Dellavalle, A., Diaz-Manera, J., et al. 2010, "Repairing skeletal muscle: regenerative potential of skeletal muscle stem cells", *The Journal of clinical investigation,* vol. 120, no. 1, pp. 11-19.

Torres-Torrillas, M., Rubio, M., Damia, E., Cuervo, B., et al. 2019, "Adipose-Derived Mesenchymal Stem Cells: A Promising Tool in the Treatment of Musculoskeletal Diseases", *International journal of molecular sciences,* vol. 20, no. 12, pp. 10.3390/ijms20123105.

Truskey, G.A. 2018, "Development and application of human skeletal muscle microphysiological systems", *Lab on a Chip,* vol. 18, no. 20, pp. 3061-3073.

Vandenburgh, H., Shansky, J., Del Tatto, M. & Chromiak, J. 1999, "Organogenesis of skeletal muscle in tissue culture", *Methods in Molecular Medicine,* vol. 18, pp. 217-225.

Wakitani, S., Saito, T., Caplan, A.I. 1995, "Myogenic cells derived from rat bone marrow mesenchymal stem cells exposed to 5-azacytidine", *Muscle & Nerve,* vol. 18, no. 12, pp. 1417-1426.

Witt, R., Weigand, A., Boos, A.M., et al. 2017, "Mesenchymal stem cells and myoblast differentiation under HGF and IGF-1 stimulation for 3D skeletal muscle tissue engineering", *BMC cell biology,* vol. 18, no. 1, pp. 15-2.

Zouraq, F.A., Stölting, M., Eberli, D. 2013, *Skeletal Muscle Regeneration for Clinical Application,* IntechOpen.

Zuk, P.A., Zhu, M., Mizuno, H., et al. 2001, "Multilineage cells from human adipose tissue: implications for cell-based therapies", *Tissue engineering,* vol. 7, no. 2, pp. 211-228.